I&EC research
Industrial & Engineering Chemistry Research

Article

Cite This: Ind. Eng. Chem. Res. 2018, 57, 15534−15541

pubs.acs.org/IECR

Effects of Protective Shell Enclosures on Uranium Adsorbing Polymers

Maha N. Haji,*[,†] Jorge Gonzalez,[†] Jessica A. Drysdale,[‡] Ken O. Buesseler,[‡] and Alexander H. Slocum[†]

[†]Department of Mechanical Engineering, Massachusetts Institute of Technology, Cambridge, Massachusetts 02139, United States
[‡]Department of Marine Chemistry & Geochemistry, Woods Hole Oceanographic Institution, Woods Hole, Massachusetts 02543, United States

ABSTRACT: This study aims to evaluate the impact of shell enclosures on the uranium uptake of amidoxime-based polymeric adsorbents contained within. Researchers have observed that the tensile strength of the adsorbent's polyethylene backbone is degraded after γ-irradiation to induce grafting of the amidoxime ligand. A two-part system was developed to decouple the mechanical and chemical requirements of the adsorbent by encapsulating them in a hard, permeable shell. The water flow in six shell designs and an unenclosed adsorbent for control in a recirculating flume was analyzed via a novel method developed using the measurement of radium extracted onto MnO_2 impregnated acrylic fibers. Although the water flow was found to vary with enclosure design, orientation to the flow, and placement within the flume, little to no difference was observed in the uranium adsorption rate between all enclosures. The results of this study will be used to design a large-scale ocean deployment of a uranium harvesting system.

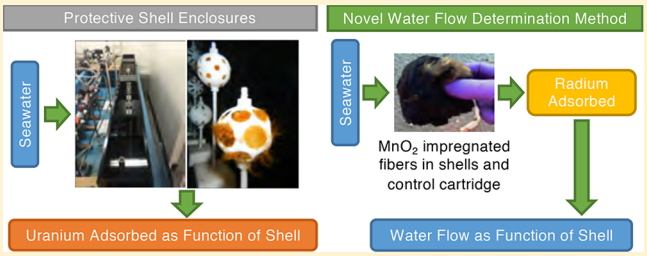

INTRODUCTION

Given that one gram of ^{235}U can theoretically produce as much energy as burning 1.5 million grams of coal,[1] nuclear power has the potential to significantly reduce carbon dioxide emissions associated with power generation. However, the approximately 7.6 million tonnes of global conventional reserves of terrestrial uranium are expected to be depleted in a little over a century at the current global consumption rate.[2] Extraction of uranium is expected to shift to lower quality sites as these reserves decrease, leading to higher extraction costs and greater environmental impacts. Fortunately, the ocean contains approximately 4.5 billion tonnes of uranium,[3] nearly 500 times more than land.

A 2013 review of uranium recovery technologies found that passive adsorption of uranium by chelating polymers was the most promising in terms of adsorbent capacity, environmental footprint, and cost.[4−7] Although developments in nanostructures materials such as metal-organic frameworks, porous-organic polymers, and mesoporous carbons, as well as inorganic materials, have shown promise in recent years, amidoxime-functionalized polymers are the most technologically mature adsorbent for this application[8] and will be the focus of the study detailed in this paper. In this technology, chelating polymers are deployed in seawater and remain submerged until the amount of captured uranium approaches the adsorption capacity. Then, the metal ions, such as uranium, are stripped off the adsorbent polymer through an elution process. A polymer may be immersed in a number of elution baths before it is regenerated by an alkali wash to free its functional groups, allowing for the redeployment and reuse of the polymer. The output from the elution process is transformed into yellowcake through a purification and precipitation process typical for terrestrially mined uranium.

In general, the amidoxime-based polymer adsorbents presented in the literature have inherently low tensile strength. For this reason, the ligands are often grafted onto a polyethylene trunk fiber that can provide high tensile strength. Research has shown that while the tensile strength of the trunk ultrahigh-molecular-weight polyethylene (UHMWPE) fiber may be more than 3.0 GPa, after γ-irradiation to induce grafting of the amidoxime ligands, this strength is decreased drastically to 1.3 GPa.[9] This decreased strength after irradiation is due to two factors. First, γ-irradiation causes the degradation of the UHMWPE molecular chain, thereby leading to a decrease in the molecular weight of polyethylene. Second, the radiation cross-linking of the UHMWPE fiber restricts the mobility of molecular chains of polyethylene and causes nonuniformity of stress in the fiber.[10,11]

Additionally, the decrease in strength after γ-irradiation was found to be dependent on the absorbed dose. The higher the radiation dose, the greater the impairment to the mechanical properties of the fibers, which influences the lifetime and recyclability of the adsorbent.[12] Thus, a method was developed to decouple the chemical and mechanical properties of the adsorbent polymer, thereby allowing for the independent

Received: July 30, 2018
Revised: September 21, 2018
Accepted: October 19, 2018
Published: October 19, 2018

DOI: 10.1021/acs.iecr.8b03583
Ind. Eng. Chem. Res. 2018, 57, 15534−15541

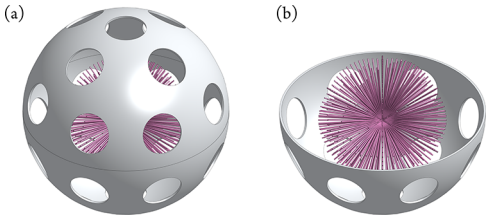

Figure 1. Initial adsorbent concept with decoupling of mechanical and chemical requirements. Soft, inner adsorbent sphere is encased in a tough, outer protective sphere. Outer sphere features holes to allow adequate seawater to adsorbent interior. Haji et al.[13] details this concept further.

optimization of both and likely leading to adsorbents with much higher adsorbent capacity.[13] In the system (shown in Figure 1), a hard permeable outer shell, with sufficient mechanical strength and durability for use in an offshore environment and chemical resilience against elution treatments, serves as the protective element for uranium adsorbent material with high adsorbent capacity. The chemistry of the inner material can thus be optimized for higher adsorption capacity, while the mechanical properties required of the system are achieved by the hard permeable outer structural shell, resulting in a system that is more cost-effective for implementation.

Previous studies have examined the effects of differing temperature,[14,15] current speed,[16] and biofouling[17] on the amidoxime-based adsorbent's ability to uptake uranium. The focus of this study is to investigate and quantify the effects, if any, of a protective shell enclosure on the uptake of uranium of the adsorbent it encapsulates. Results obtained from this study will provide critical information in determining the types of protective shell enclosures to be used in a large-scale ocean test of a uranium harvesting system, such as that detailed by Haji et al.[18]

METHODOLOGY

Recirculating Flume Experimental Setup. To investigate the effects of encasing an adsorbent in a shell enclosure on the uranium it adsorbs, six shell enclosure designs were developed for testing. The shell designs were tested in a recirculating flume tank located at the Woods Hole Oceanographic Institution's (WHOI) Shore Lab. The tank allowed ambient 0.45 μm filtered seawater to pass through the shells continuously. The flume measured 1.83 m × 0.15 m × 0.3 m and was constructed using 1.27 cm (0.5 in) dark colored acrylic. The dark colored opaque acrylic prevented light from passing through, thereby mitigating the effects of biofouling.[17] Fresh filtered seawater, with temperature held at 20 ± 1.5 °C, was fed into the system from the head tank at flow-rates up to 3 L/min, resulting in a water residence time of ∼21 min. As fresh seawater was pumped into the flume, a 23 cm stand pipe near the recirculation outlet ensured the water level in the flume remained at a constant level. An inlet and outlet allowed the seawater within the flume to be recirculated at a constant flow rate. A diagram of the flume experiment is shown in Figure 2.

A Finnish Thompson DB8 centrifugal, nonmetallic, pump recirculated seawater in the flume at a rate of 100 L/min, corresponding to a linear flow rate in the flume of 4.8 cm/s. At this rate, the water in the flume was recirculated once every 38 s. The flow rate was regulated using a globe valve positioned after the pump's discharge port. The volumetric flow rate was continuously monitored using an Omega FP2010-RT flow meter in line between the recirculation outlet and the pump.

To ensure that no shell enclosure was in the wake of another, the six shell enclosures were staggered in their vertical placement in the flume. A seventh threaded rod and block served as an attachment point for an unenclosed piece of adsorbent that served as the control. A baffle, made of stacked 1.27 cm (0.5 in) PVC pipe segments and installed near the recirculation inlet of the flume, minimized turbulence as the flow approached the shell enclosures.

A digital pressure meter was used to measure the pressure before the recirculation inlet and after the recirculation outlet to determine the pressure loss across the flume. The pressures were found to be 28.27 and 27.58 kPa respectively, indicating a negligible pressure loss of 0.69 kPa (∼2.4%) across the flume and confirming that the flow meter's measurement would not be affected by the pressure drop. The pump, flow meter, and all piping components were chosen such that all wetted components were made of plastic, thereby minimizing the possibility of contaminating the adsorbents with other metal ions.

Design Analysis. The shell diameter and locations within the flume were chosen to ensure the shells would not lie in the boundary layer created by the walls of the flume or in the wake created by shells upstream. The free stream velocity, u, is given by the volumetric flow rate, Q, divided by the cross sectional area of the flume:

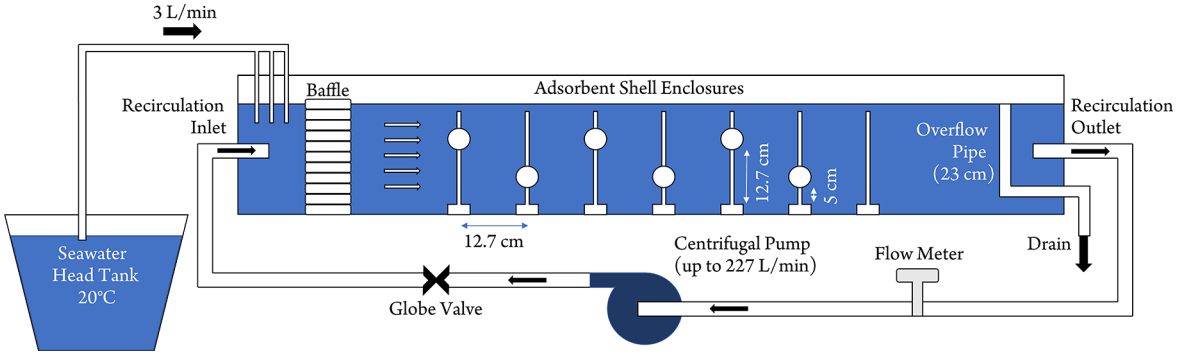

Figure 2. Diagram of the recirculating flume setup used to test the shell enclosures. Fresh seawater is pumped in from a head tank using three tubes near the recirculation inlet. Overflow pipe ensures a constant water level of 23 cm. A Finish Thompson DB8 Centrifugal Pump constantly recirculates the filtered seawater.

DOI: 10.1021/acs.iecr.8b03583
Ind. Eng. Chem. Res. 2018, 57, 15534−15541

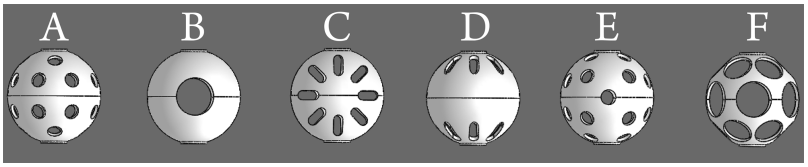

Figure 3. Solid models of six shell designs selected for testing in order of placement in the recirculating flume (with design A being closest to the inlet).

Figure 4. (a) MnO_2 impregnated acrylic fibers used in this study, (b) the ashing process showing one clump of MnO2 impregnated acrylic fiber in a container ready for ashing, and (c) samples in a muffle furnace prior to ashing.

$$u = \frac{Q}{w_f d_f} \tag{1}$$

where w_f is the width of the flume and d_f is the depth of the water filling the flume. The flow regime at any point in the flume can be determined from the local Reynolds number, given by

$$\mathrm{Re}(x) = \frac{ux}{\nu} \tag{2}$$

where $\mathrm{Re}(x)$ is the local Reynolds number, u is the free stream velocity, x is the distance downstream from the boundary layer, and ν is the kinematic viscosity of seawater.

Since the fluid's velocity asymptotically approaches the free stream velocity, the thickness of the boundary layer is commonly taken as the point where the fluid velocity equals 99% of the free stream velocity. From eq 2, it was found that any free stream velocity greater than 0.92 cm/s resulted in a nonlaminar flow regime within the flume, for which the boundary layer thickness is then given by

$$\delta = \frac{0.382x}{\mathrm{Re}(x)^{1/5}} \tag{3}$$

where δ is the boundary layer thickness, x is the distance downstream from the start of the inlet, and $\mathrm{Re}(x)$ is the local Reynolds number.[19]

For a flow rate of 4.8 cm/s, as was used in this experiment, and a shell spacing of 12.7 cm, the boundary layer at the last shell would be approximately 45 mm thick (on either side of the tank walls). This indicates that the flow in and around a shell with a diameter greater than 62 mm would be affected by the boundary layers from the flume tank walls. Hence, a shell with a diameter of 50 mm was selected for use in this experiment.

Shell Enclosure Design and Fabrication. Of the six shell enclosure designs developed for testing, one was based on a classic wiffle ball with holes, which contained 24 holes positioned in four different tiers around the shell. Another design was based on a classic wiffle ball with slotted holes, containing eight slotted holes arranged in a circular pattern on each side of the shell. Figure 3 shows the six shell designs tested in this study in the order they were placed in a recirculating flume (with A being the closest to the inlet) as well as the naming convention used in the discussion. Enclosures A and E are the same design (the holed wiffle), with the exception that they have different orientations to the flow. The same is true for enclosures C and D.

The shells were fabricated in two halves and included a series of tabs and corresponding slots that allowed the two halves to be aligned each time they are connected. Each half shell was 50 mm in diameter and 3D printed from white acrylic. Acrylic, unlike some other plastics, will not absorb water or deform after being submerged in seawater for extended periods of time. Unlike colored acrylics, white acrylic does not contain any added dyes that could potentially leach into the seawater and affect the fibers' uptake of uranium.

The fabricated shell enclosures included holes for a 0.63 cm (0.25 in) diameter threaded acetal rod. Each half shell was secured to the threaded rod with two nylon nuts. The threaded rod was then inserted into an acetal block which was glued to the base of the recirculating flume tank.

Water Flow Measurement. To determine if the shell designs impeded the water flow to the adsorbent interior (and therefore possibly hindered the uptake of the uranium adsorbing fibers enclosed), a novel method using the collection and measurement of radium extracted onto MnO_2 impregnated acrylic fibers was used to quantify the volume of water passing through the fibers in each of the different types of enclosures, including the control.

Radium is an alkaline earth metal, and each of its four isotopes is produced by the decay of their radiogenic parents. Although each of the four have different half-lives (^{226}Ra, $t_{1/2}$ = 1,600 years; ^{228}Ra, $t_{1/2}$ = 5.75 years; ^{223}Ra, $t_{1/2}$ = 11.4 days; and ^{224}Ra, $t_{1/2}$ = 3.66 days), they exhibit similar physicochemical properties.[20] In seawater, radium isotopes exist in dissolved form,[21−23] move with the water body, and are transported in the ocean by advective and diffusive mixing processes. Given its suitability as a tracer for water masses in oceanographic studies,[24−29] radium is used in this study in a novel way to evaluate the water mass encountered by fibers within the various shell enclosures and the control. To the authors' knowledge, this use of radium to quantify water flow has not been documented in the literature and represents an additional contribution of this work.

The MnO_2 impregnated acrylic fiber (Figure 4(a)) was prepared by immersing an acrylic fiber into a 0.5 mol $KMnO_4$

DOI: 10.1021/acs.iecr.8b03583
Ind. Eng. Chem. Res. 2018, 57, 15534−15541

solution heated to 75° where it remained until the fiber turned black. The fiber was then removed and rinsed thoroughly using radium free deionized water until the water ran clear.[30] Fibers were then air-dried and weighed prior to use.

The MnO_2 impregnated acrylic fibers, which adsorb radium, were placed in a control, and in each of the different types of enclosures including on a threaded acetal rod with no enclosure to act as a control. The fibers were tested in the flume for approximately 6.25 h. At the same time, seawater that recirculated into the flume was also used to fill a 120 L container that was then slowly pumped through the cartridge at about 1−2 L/min (a rate below 2 L/min has been shown to achieve quantitative radium adsorption[30,31]).

After the seawater exposure, following the method of Moore (1984),[32] the fibers were ashed in a muffle furnace at 820 °C for 24 h (Figures 4(b) and (c)), resulting in a mass reduction of up to 60%. The ash was then concealed in epoxy resin to contain Ra gases. After a three-week waiting period, which allows all daughters of ^{226}Ra to grow into equilibrium, the samples were counted for ^{226}Ra using γ-spectrometry by its photopeak at 352 keV. The known volume of water filtered through the cartridge and the amount of radium adsorbed by the fiber in the cartridge was used to determine a relationship between the radium adsorbed and total volume of seawater to come in contact with the adsorbent fiber.

Adsorbent Preparation and Sampling. The designs described in this paper utilized the AI8 adsorbent developed at Oak Ridge National Laboratory (ORNL) (originally named the AI11 adsorbent, detailed further in Das et al.[33]). Adsorbents were prepared using hollow-gear-shaped, high-surface-area polyethylene fibers and a radiation-induced graft polymerization method.[34] The AI8 adsorbent uses vinylphosphonic acid as the grafting comonomer and amidoxime as the uranium binding ligand. The uranium uptake of this adsorbent can be calculated using the one-site ligand-saturation model. In this model, the uranium uptake, y, after a certain exposure time in days, t, is given by

$$y = \frac{\beta_{\max} t}{K_D + t} \tag{4}$$

where β_{max} is the saturation capacity in g U/kg adsorbent, and K_D is the half-saturation time in days.[33]

Each shell contained a preweighed, small mass (~3 g) of adsorbent fiber (Figure 5) cut from a common AI8 adsorbent braid prepared by ORNL.[35] Additionally, some adsorbent was tied to a threaded acetal rod with no enclosure to act as a control. Samples were collected after the first 24 h and then again once per week for 8 weeks, for a total of nine samples over 56 days. Samples were taken by snipping small pieces (~35 mg) using Teflon coated scissors from sections of the adsorbent fiber in each enclosure and from the control.

Uranium and Trace Element Analysis. After exposure to seawater in the recirculating flume, the adsorbent samples were analyzed at the Marine Sciences Lab at Pacific Northwest National Laboratory (PNNL) for uranium and other trace elements. The samples were first rinsed in deionized water to remove accumulated salts. Then each sample was placed in a plastic vial and dried overnight using a heating block at 80 °C after which the dried adsorbent sample was weighed. Total digestion of the adsorbent was achieved by placing the sample in a 50% aqua regia solution and incubated for 2 h in a heating block at 80 °C. The sample was then analyzed for uranium and trace elements via inductively coupled plasma optical emission spectrometry. Adsorption (uptake) was determined based on the mass of the recovered elements per mass of adsorbent (g of element adsorbed per kg of dry adsorbent).

Figure 5. Shell enclosures in the recirculating flume, each containing a small, preweighed, mass of adsorbent fiber. Samples were taken by snipping small pieces (~35 mg) using Teflon coated scissors from sections of the adsorbent fiber in each enclosure and from the control.

In addition to adsorbent samples, water samples were also collected on each of the nine sample dates for trace metal analysis. Furthermore, salinity measurements were taken using a YSI Pro30 Conductivity Probe as salinity has been shown to indicate the ^{238}U concentration in seawater. The concentration of ^{238}U in (ng g^{-1}) is described as

$$^{238}\mathrm{U}(\pm 0.061) = 0.100 \times S - 0.326 \tag{5}$$

where S is the salinity.[36]

RESULTS

Water Flow through Shells. Figure 6 shows the results of the water flow in the different shells after correcting for the differences in the amount of radium fibers initially placed in each of the enclosures and adjusting for weight due to ash loss.

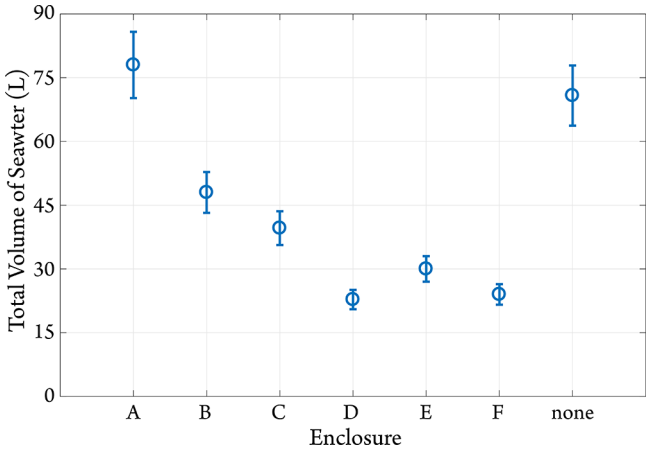

Figure 6. Total volume of seawater to come in contact with MnO_2 impregnated acrylic fibers in different enclosure types as determined by ^{226}Ra count using γ-spectrometry.

DOI: 10.1021/acs.iecr.8b03583
Ind. Eng. Chem. Res. 2018, 57, 15534−15541

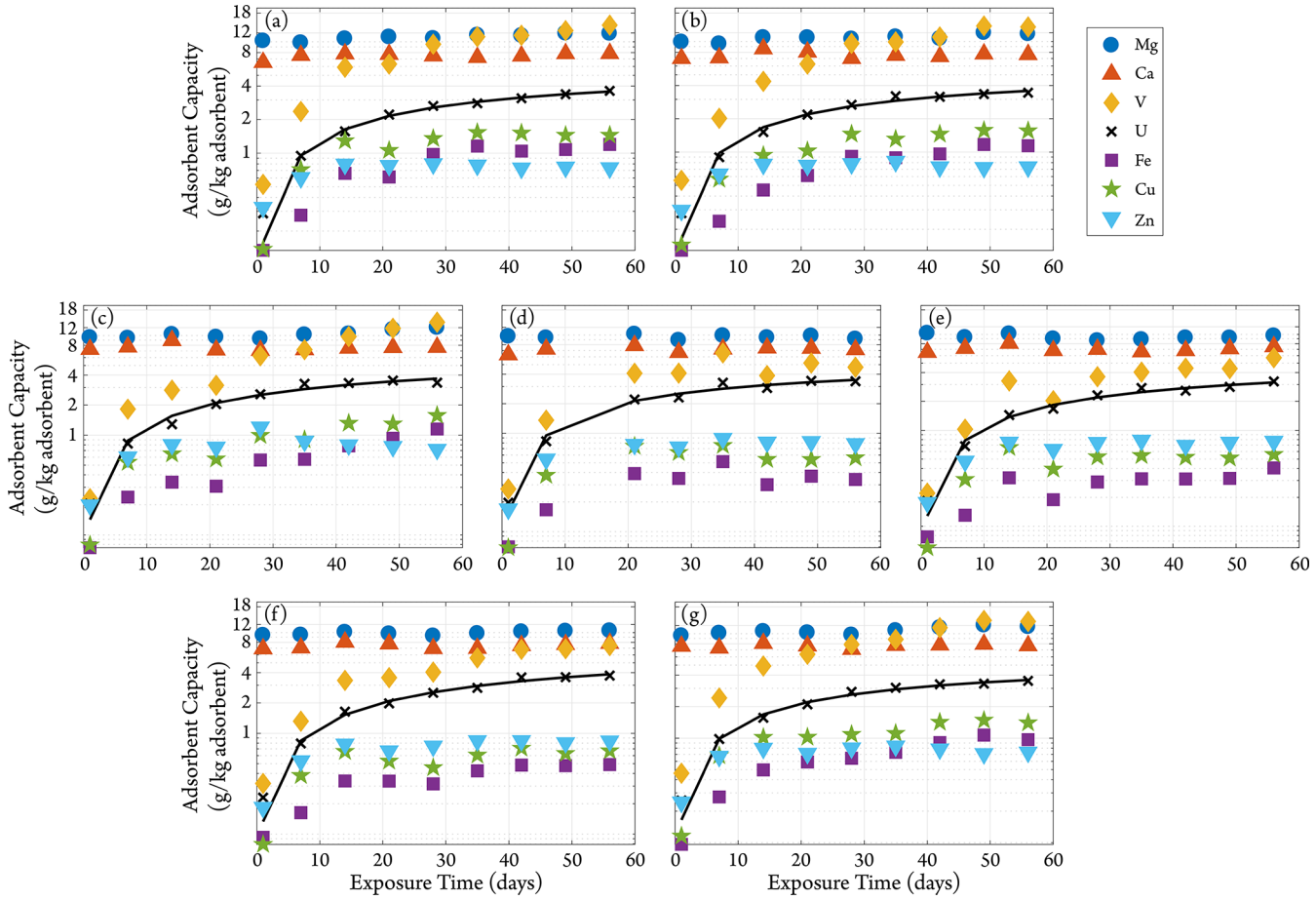

Figure 7. Time-dependent measurements of adsorption capacities (g element/kg adsorbent) for several trace elements retained by the ORNL AI8 adsorbent exposed to filtered natural seawater in a flume in various shell enclosures, (a)−(f) (as shown in Figure 3), and without any enclosure, (g). The black line drawn through the uranium adsorption data represents fitting to a one-site ligand model (eq 4).

The results indicate that there was a significant difference in the water passing within the enclosures. In particular, the shell enclosure closest to the baffle, A, saw the most water, about the same as the unenclosed control fiber. Additionally, the total volume of seawater the adsorbent came in contact with seemed to taper off farther down the flume, with enclosures D, E, and F seeing less flow than enclosures B and C. Specifically, the fiber in enclosure D saw over 60% less water than the control fiber without an enclosure. The water flow to the fiber in enclosures A and E (the same shell design oriented differently to the flow) differed by over 60%. Similarly, there was over 42% difference in the water flow to the fiber in enclosures C and D.

Although the shells were placed in the flume in such a way as to ensure no shell was in the wake of those preceding it, the results from the radium analysis indicated that the total water seen by the adsorbent in shells farther down the flume was reduced as compared to enclosure A and the control (no enclosure). This may have been due to the fact that the shells were observed to vibrate in the flow. Eddies formed on either side of the shells may have started alternating, producing an oscillation and resulting in vortex induced vibrations. The vibration may have varied from shell to shell as each shell may have been influenced by vortices from preceding shells, thereby changing the water flow based on a shell's placement within the flume. Given that the control adsorbent fiber was not encapsulated, it did not experience such vibrations.

These results suggest that the design of the shell enclosure, the orientation of the shell enclosures with respect to the incoming flow, and the placement of the shell within the flume had a significant effect on the amount of water flow to the interior and could indicate an effect on the amount of uranium adsorbed by the fibers enclosed by each shell.

Uranium Uptake. The salinity during the experiment averaged 32.6 ± 0.2 psu, indicating an average ^{238}U concentration by eq 5 of 2.934 ± 0.081 ppb. Due to the conservative behavior of uranium in seawater,[37] all uranium adsorption capacity data was normalized to a salinity of 35 psu in order to correct for the varying salinity of natural seawater observed in different adsorption experiments. Adsorption kinetics and saturation capacity were determined by fitting time-dependent measurements of adsorption capacity using a one-site ligand saturation model as described by eq 4. Figure 7 shows the time-dependent measurements of adsorption capacities for all trace metals retained by the AI8 adsorbent for each enclosure. As can be seen, uranium is not the dominant metal adsorbed by the fiber.

The uranium adsorption capacity (g-U/kg-adsorbent) for all adsorbents in all the enclosures is shown in Figure 8, with the lines indicating the one-site ligand saturation model fits for each enclosure. There is very little difference in the uranium adsorbed between the different enclosure types. This is further confirmed by the kinetic parameters of the one-site ligand model, detailed in Table 1. Detailed are the uptake predicted

DOI: 10.1021/acs.iecr.8b03583
Ind. Eng. Chem. Res. 2018, 57, 15534−15541

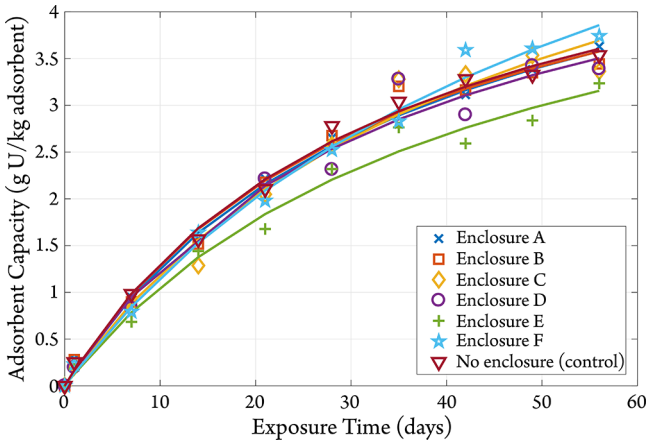

Figure 8. Time-dependent measurements of uranium adsorption capacity (g-U/kg-adsorbent) for the flume experiment for the seven AI8 adsorbent braids enclosed by various shell designs (Enclosures A−F), as well as the results from the control adsorbent in no enclosure. The uranium adsorption capacity was normalized to a salinity of 35 psu. Curves drawn through the data represent fitting to eq 4, the one-site ligand model. Table 1 details the saturation capacity and half-saturation times as predicted from the one-site ligand model fits.

Table 1. Uranium 56-day Adsorption Loadings (56-d, g U/kg adsorbent), Saturation Capacities (β_{max}, g U/kg adsorbent), and Half-Saturation Time (K_D, days) for the AI8 Adsorbents Enclosed by Different Shell Designs (Enclosures A−F), and a Control Adsorbent in No Enclosure[a]

Enclosure	56-d[b]	β_{max}[b]	K_D[b]
A	3.58 ± 0.93	5.91 ± 0.69	36.55 ± 8.51
B	3.58 ± 1.65	5.57 ± 1.16	33.99 ± 14.13
C	3.70 ± 2.91	6.78 ± 2.59	46.67 ± 32.15
D	3.50 ± 3.06	5.67 ± 2.14	34.69 ± 27.36
E	3.16 ± 1.93	5.55 ± 1.60	42.40 ± 22.87
F	3.86 ± 2.13	7.84 ± 2.23	57.83 ± 27.38
No enclosure (control)	3.60 ± 1.26	5.80 ± 0.89	34.17 ± 10.76

[a]Adsorption loadings were normalized to a salinity of 35 psu. [b]Estimated using the one-site ligand saturation model (eq 4).

for an immersion time of 56 days as determined from the one-site ligand model, the saturation capacity, β_{max}, and half saturation time, K_D, with the ±95% confidence intervals. As seen in the table, little variability exists between the coefficients of the fits for each shell enclosure, suggesting no significant difference in the uranium uptake by the adsorbent in different shell enclosures.

The results suggest that even though the flow field inside the shell enclosures may have differed considerably,[38] the enclosure is likely not inhibiting the uranium adsorption of the fibers it encases, no matter the shell design. The lack of difference in uranium uptake between shell enclosures suggests that the linear velocity of the water is high enough that the reaction is no longer mass limited. Such a result was also observed by Ladshaw et al.[16] for similar linear velocities. Variations in the mass-transfer rates depend on the linear velocity as well as the form-factor of the adsorbent.[16] The enclosures and the high linear velocity flow used in this experiment result in less freely fluidized adsorbent fibers than if the adsorbent was submerged unenclosed in slowly agitated seawater, as in Kim et al.[39] Because of this, the speed of interparticle diffusion (the transport of adsorbate from bulk liquid phase to the exterior film of the adsorbent) is likely reduced as compared to experiments performed by Kim et al. (2013). While the external mass-transfer resistance has not been successfully removed, as suggested by Ladshaw et al.,[16] it may not be enough to make the interparticle diffusion transport mechanism the rate limiting step of the uranium uptake process.

Most of the other elements shown in Figure 7 indicate similar trends between all enclosures. The consistent concentrations of calcium (Ca) and magnesium (Mg) may be a result of salts on the fibers rather than adsorption, though Ca and Mg have been show to bind weakly to amidoxime.[40] Vanadium (V), iron (Fe), copper (Cu), and zinc (Zn), on the other hand, may adsorb to the amidoxime and may displace or prevent uranium adsorption.[41] As with uranium adsorption in this study, the adsorption of Fe, Cu, and Zn does not seem to vary between enclosures, supporting the results that the enclosures do not affect the adsorption kinetics of the fibers they encapsulate. V, on the other hand, shows increased adsorption on fibers in enclosures A, B, C (Figure 7(a)−(c)) and the fiber control, (Figure 7(g)). It has been shown that vanadium outcompetes other ions, including uranium, for adsorption, though the binding method remains unclear.[35,42] This suggests that the increased vanadium adsorption could have limited the fiber's adsorption of uranium, supporting the idea that in the absence of vanadium, the uranium adsorption may have been increased in enclosures A, B, C and the control. Given that enclosure F had the largest holes and most open area of any enclosure, this suggestion is quite surprising. To investigate this idea further, future studies should use a single shell enclosure design placed at various locations in the flume with samples being taken at each location to eliminate the possibility that placement within the flume could have caused these variations in trace metal uptake.

CONCLUSION

This paper presented the results of an experiment to determine the effect of shell enclosures on the uptake of uranium by adsorbent fibers they encapsulate. Six designs of shell enclosures were tested in a recirculating seawater flume at WHOI. The design and fabrication of these shells was described in detail. Analysis was presented to ensure negligible boundary layer effects on the shells in the flume.

A novel method for water flow measurement was developed using MnO_2 impregnated acrylic fibers, which adsorb radium, to determine the water flow inside each shell. Through comparison of the radium adsorption of these fibers to that of fibers in a control cartridge, the total volume of seawater the adsorbent came in contact with in each enclosure was determined.

Next, the experimental procedure was described. The AI8 adsorbent fiber developed by ORNL was enclosed in each shell, and some fiber was included in the flume without any enclosure to act as a control. Nine samples of the fiber and water samples from the flume were collected over a period of 56-days. Postexposure, the fibers were analyzed by PNNL for uranium and other trace elements.

The results from this experiment will help inform the types of protective shell enclosures to be used in a large-scale ocean test of a uranium harvesting system, such as that detailed by Haji et al.[18] It has been suggested that uranium harvesting

DOI: 10.1021/acs.iecr.8b03583
Ind. Eng. Chem. Res. 2018, 57, 15534−15541

systems be deployed in the ocean within eastern boundary currents, which can range from 10 to 30 cm/s, in order to maximize water flow by the adsorbent. However, Ladshaw et al.[16] recommend to minimize mass-transfer resistances and maximize adsorbent capacities, adsorbent fibers should be deployed in ocean currents greater than 8 cm/s, which could be produced by a wind speed of 400 cm/s,[43] a mild speed that occurs in many regions of the ocean. At a flow rate of 4.8 cm/s used in this experiment, much lower than that recommended by Ladshaw et al.,[16] the shell enclosures were found to have no negative impact on the uranium adsorption of fibers they encapsulate, suggesting that the shell design chosen for an ocean test will also have minimal effect on the fiber's uptake. The study presented in this paper followed identical methods to those used at PNNL[44] and described in Ladshaw et al.[16] In brief, adsorption capacity was obtained by cutting a small mass (~35 mg) from sections of the braided material. Replicate measurements taken from the adsorbents agree very well, but the dense core material has been shown to have a much lower and much more variable uranium concentration,[35] and thus this sampling bias may have introduced differences in this study in comparison to the study of Ladshaw et al.[16]

Additional experiments should investigate how the adsorbent fiber may survive in harsh ocean conditions. Biofouling of adsorbent fibers can have an adverse effect on uranium uptake,[17] and future work should examine the effects of adsorbent shell enclosures on the biofouling of adsorbent fibers. Additionally, this experiment used filtered seawater whereas in the open ocean biofouling on the shell enclosures themselves may interfere with the ability of water to flow in, and hence reduce uranium uptake. This is the topic of a further ocean experiment, the results of which are detailed in Haji et al.[45]

To eliminate the possibility that placement within the flume could have caused the resulting variations in trace metal adsorption, future studies should use a single shell enclosure placed at various locations in the flume with samples being taken at each location. Lastly, further structural analysis of protective shell enclosures used in this experiment should be conducted to determine the effects of distributed and point loads on different shell geometries.

AUTHOR INFORMATION

Corresponding Author

*E-mail: mhaji@mit.edu.

ORCID

Maha N. Haji: 0000-0002-2953-7253

Notes

The authors declare no competing financial interest.

ACKNOWLEDGMENTS

This work was supported by the U.S. Department of Energy Office of Nuclear Energy under Contracts No. DE-NE0008268 and DE-NE000731 and by the National Academies Keck Futures Initiative. This material is based upon work supported by the National Science Foundation Graduate Research Fellowship under Grant No. 1122374. Any opinion, findings, and conclusions or recommendations expressed in this material are those of the authors and do not necessarily reflect the views of the National Science Foundation. The authors thank Oak Ridge National Laboratory for the preparation of the adsorbent fibers for use in this study and G. Gill and other researchers at the Pacific Northwest National Laboratory for the analysis of the fibers postexposure.

REFERENCES

(1) Emsley, J. *Nature's Building Blocks: An A to Z. Guide to the Elements*; Oxford University Press, 2001; pp 476–482.

(2) OECD Nuclear Energy Agency. *Uranium 2016: Resources, Production and Demand*; 2016.

(3) Oguma, K.; Suzuki, T.; Saito, K. Determination of uranium in seawater by flowinjection preconcentration on dodecylamidoxime-impregnated resin and spectrophotometric detection. *Talanta* **2011**, *84*, 1209–1214.

(4) Kim, J.; Tsouris, C.; Mayes, R. T.; Oyola, Y.; Saito, T.; Janke, C. J.; Dai, S.; Schneider, E.; Sachde, D. Recovery of Uranium from Seawater: A Review of Current Status and Future Research Needs. *Sep. Sci. Technol.* **2013**, *48*, 367–387.

(5) Zhang, A.; Asakura, T.; Uchiyama, G. The adsorption mechanism of uranium (VI) from seawater on a macroporous fibrous polymeric adsorbent containing amidoxime chelating functional group. *React. Funct. Polym.* **2003**, *57*, 67–76.

(6) Seko, N.; Katakai, A.; Hasegawa, S.; Tamada, M.; Kasai, N.; Takeda, H.; Sugo, T.; Saito, K. Aquaculture of uranium in seawater by a fabric-adsorbent submerged system. *Nucl. Technol.* **2003**, *144*, 274–278.

(7) Anirudhan, T. S.; Tharun, A. R.; Rijith, S.; Suchithra, P. S. Synthesis and characterization of a novel graft copolymer containing carboxyl groups and its application to extract uranium (VI) from aqueous media. *J. Appl. Polym. Sci.* **2011**, *122*, 874–884.

(8) Abney, C. W.; Mayes, R. T.; Saito, T.; Dai, S. Materials for the Recovery of Uranium from Seawater. *Chem. Rev.* **2017**, *117*, 13935–14013.

(9) Xing, Z.; Hu, J.; Wang, M.; Zhang, W.; Li, S.; Gao, Q.; Wu, G. Properties and evaluation of amidoxime-based UHMWPE fibrous adsorbent for extraction of uranium from seawater. *Sci. China: Chem.* **2013**, *56*, 1504–1509.

(10) Yamanaka, A.; Izumi, Y.; Kitagawa, T.; Terada, T.; Hirahata, H.; Ema, K.; Fujishiro, H.; Nishijima, S. The effect of gamma-irradiation on thermal strain of high strength polyethylene fiber at low temperature. *J. Appl. Polym. Sci.* **2006**, *102*, 204–209.

(11) Zhao, Y. N.; Wang, M. H.; Tang, Z. F.; Wu, G. Z. Effect of gamma-ray irradiation on the structure and mechanical properties of UHMWPE fibers. *Polymer Materials Science & Engineering* **2010**, *26*, 32–35.

(12) Hu, J.; Ma, H.; Xing, Z.; Liu, X.; Xu, L.; Li, R.; Ling, C.; Wang, M.; Li, J.; Wu, G. Preparation of Amidoximated UHMWPE Fiber by Radiation Grafting and Uranium Adsorption Test. *Ind. Eng. Chem. Res.* **2016**, *55*, 4118

(13) Haji, M. N.; Vitry, C.; Slocum, A. H. Decoupling the functional requirements of an adsorbent for harvesting uranium from seawater through the use of shell enclosure. *Transactions of the American Nuclear Society* **2015**, *113*, 158–161.

(14) Ladshaw, A.; Wiechert, A. I.; Das, S.; Yiacoumi, S.; Tsouris, C. Amidoxime Polymers for Uranium Adsorption: Influence of Comonomers and Temperature. *Materials* **2017**, *10*, 1268.

(15) Kuo, L.-J.; Gill, G. A.; Tsouris, C.; Rao, L.; Pan, H.-B.; Wai, C. M.; Janke, C. J.; Strivens, J. E.; Wood, J. R.; Shlafer, N.; D'Alessandro, E. K. Temperature Dependence of Uranium and Vanadium Adsorption on Amidoxime-Based Adsorbents in Natural Seawater. *Chemistry Select* **2018**, *3*, 843–848.

(16) Ladshaw, A.; Kuo, L.-J.; Strivens, J.; Wood, J.; Schlafer, N.; Yiacoumi, S.; Tsouris, C.; Gill, G. Influence of Current Velocity on Uranium Adsorption from Seawater Usingan Amidoxime-Based Polymer Fiber Adsorbent. *Ind. Eng. Chem. Res.* **2017**, *56*, 2205–2211.

(17) Park, J.; Gill, G. A.; Strivens, J. E.; Kuo, L.-J.; Jeters, R.; Avila, A.; Wood, J.; Schlafer, N. J.; Janke, C. J.; Miller, E. A.; Thomas, M.; Addleman, R. S.; Bonheyo, G. Effect Of Biofouling On The Performance Of Amidoxime-Based Polymeric Uranium Adsorbents. *Ind. Eng. Chem. Res.* **2016**, *55*, 4328

DOI: 10.1021/acs.iecr.8b03583
Ind. Eng. Chem. Res. 2018, 57, 15534–15541

(18) Haji, M. N.; Slocum, A. H. Design of a Symbiotic Device to Harvest Uranium from Seawater through the use of Shell Enclosures. *Transactions of the American Nuclear Society* **2016**, *115*, 153−156.
(19) Schlichting, H. *Boundary-layer theory*, 7th ed.; McGraw-Hill: New York, 1979; p 634.
(20) Zhang, L.; Zhang, J.; Swarzenski, P. W.; Liu, Z. In *Handbook of Environmental Isotope Geochemistry*; Baskaran, M., Ed.; Springer, 2011; Chapter 17, pp 331−343.
(21) Moore, W. S. Radium isotopes in the Chesapeake Bay. *Estuarine, Coastal Shelf Sci.* **1981**, *12*, 713−723.
(22) Key, R. M.; Stallard, R. F.; Moore, W. S.; Sarmiento, J. L. Distribution and flux of ^{226}Ra and ^{228}Ra in the Amazon River estuary. *J. Geophys. Res.* **1985**, *90*, 6995−7004.
(23) Moore, D. G.; Scoot, M. R. Behavior of ^{226}Ra in the Mississippi River mixing zone. *J. Geophys. Res.* **1986**, *91*, 14317−14329.
(24) Moore, W. S. Large ground water inputs to coastal waters revealed by ^{226}Ra enrichments. *Nature* **1996**, *380*, 612−614.
(25) Rama; Moore, W. S. Using the radium quartet to estimate water exchange and ground water input in salt marshes. *Geochim. Cosmochim. Acta* **1996**, *60*, 4645−4652.
(26) Moore, W. S.; Sarmiento, J. L.; Key, R. M. *J. Geophys. Res.* **1986**, *91*, 2574−2580.
(27) Moore, W. S.; Todd, J. F. Radium isotopes in the Orinoco estuary and eastern Caribbean Sea. *Journal of Geophysical Research* **1993**, *98*, 2233−2244.
(28) Kim, G.; Ryu, J. W.; Yang, H. S.; Yun, S. T. Submarine groundwater discharge (SGD) into the Yellow Sea revealed by ^{228}Ra and ^{226}Ra isotopes: implications for global silicate fluxes. *Earth Planet. Sci. Lett.* **2005**, *237*, 156−166.
(29) Moore, W. S.; Blanton, J. O.; Joyce, S. B. Estimates of flushing times, submarine groundwater discharge, and nutrient fluxes to Okatee Estuary, South Carolina. 2006, DOI: 10.1029/2005JC003041.
(30) Moore, W. S. Sampling ^{228}Ra in the deep ocean. *Deep-Sea Res. Oceanogr. Abstr.* **1976**, *23*, 647−651.
(31) Moore, W. S.; Astwood, H.; Lindstrom, C. Radium isotopes in coastal waters on the Amazon shelf. *Geochim. Cosmochim. Acta* **1995**, *59*, 4285−4298.
(32) Moore, W. S. Radium isotope measurements using germanium detectors. *Nucl. Instrum. Methods Phys. Res.* **1984**, *223*, 407−411.
(33) Das, S.; Oyola, Y.; Mayes, R. T.; Janke, C. J.; Kuo, L.-J.; Gill, G.; Wood, J. R.; Dai, S. Extracting Uranium from Seawater: Promising AI Series Adsorbents. *Ind. Eng. Chem. Res.* **2016**, *55*, 4103−4109.
(34) Kim, J.; Tsouris, C.; Oyola, Y.; Janke, C. J.; Mayes, R. T.; Dai, S.; Gill, G.; Kuo, L.-J.; Wood, J.; Choe, K.-Y.; Schneider, E.; Lindner, H. Uptake of uranium from seawater by amidoxime-based polymeric adsorbent: Field experiments, modeling, and updated economic assessment. *Ind. Eng. Chem. Res.* **2014**, *53*, 6076−6083.
(35) Gill, G. A.; Kuo, L.-J.; Janke, C. J.; Park, J.; Jeters, R. T.; Bonheyo, G. T.; Pan, H.-B.; Wai, C.; Khangaonkar, T.; Bianucci, L.; Wood, J. R.; Warner, M. G.; Peterson, S.; Abrecht, D. G.; Mayes, R. T.; Tsouris, C.; Oyola, Y.; Strivens, J. E.; Schlafer, N. J.; Addleman, R. S.; Chouyyok, W.; Das, S.; Kim, J.; Buesseler, K.; Breier, C.; D'Alessandro, E. The Uranium from Seawater Program at the Pacific Northwest National Laboratory: Overview of Marine Testing, Adsorbent Characterization, Adsorbent Durability, Adsorbent Toxicity, and Deployment Studies. *Ind. Eng. Chem. Res.* **2016**, *55*, 4264−4277.
(36) Owens, S. A.; Buesseler, K. O.; Sims, K. W. W. Re-evaluating the ^{238}U-salinity relationship in seawater: Implications for the ^{238}U-Th- 234 disequilibrium method. *Mar. Chem.* **2011**, *127*, 31−39.
(37) Not, C.; Brown, K.; Ghaleb, B.; Hillaire-Marcel, C. Conservative behavior of uranium vs. salinity in Arctic sea ice and brine. *Mar. Chem.* **2012**, *130−131*, 33−39.
(38) Hamlet, A. M. Uranium Extraction from Seawater: Investigating the Hydrodynamic Behavior and Performance of Porous Shells. M.Sc. thesis, Massachusetts Institute of Technology, 2017.
(39) Kim, J.; Oyola, Y.; Tsouris, C.; Hexel, C. R.; Mayes, R. T.; Janke, C. J.; Dai, S. Characterization of uranium uptake kinetics from seawater in batch and flow-through experiments. *Ind. Eng. Chem. Res.* **2013**, *52*, 9433−9440.
(40) Leggett, C.; Rao, L. Complexation of calcium and magnesium with glutarimidedioxime: Implications for the extraction of uranium from seawater. *Polyhedron* **2015**, *95*, 54−59.
(41) Kuo, L.-J.; Janke, C. J.; Wood, J. R.; Strivens, J. E.; Das, S.; Oyola, Y.; Mayes, R. T.; Gill, G. A. Characterization and Testing of Amidoxime-Based Adsorbent Materials to Extract Uranium from Natural Seawater. *Ind. Eng. Chem. Res.* **2016**, *55*, 4285−4293.
(42) Abney, C.; Mayes, R.; Piechowicz, M.; Lin, Z.; Bryantsev, V.; Veith, G.; Dai, S.; Lin, W. XAFS investigation of polyamidoxime-bound uranyl contests the paradigm from small molecule studies. *Energy Environ. Sci.* **2015**, *9*, 448−453.
(43) Gross, M. G. *Oceanography - A view of Earth*, 6th ed.; Prentice Hall: Englewood Hills, NJ, 1993.
(44) Gill, G. A.; Kuo, L.-J.; Strivens, J.; Wood, J.; Schlafer, N. J.; Tsouris, C.; Ladshaw, A.; Yiacoumi, S. Investigations into the Effect of Current Velocity on Amidoxime-Based Polymeric Uranium Adsorbent Performance, Milestone Report: PNNL-SA-24996. *U. S. Department of Energy* **2015**. DOI: 10.2172/1332628
(45) Haji, M. N.; Drysdale, J.; Buesseler, K.; Slocum, A. Results of Ocean Trial of a Symbiotic Device to Harvest Uranium from Seawater through the Use of Shell Enclosures. Submitted to *Environ. Sci. Technol.* **2018**.

DOI: 10.1021/acs.iecr.8b03583
Ind. Eng. Chem. Res. 2018, 57, 15534−15541